Journal of Interfaces, Thin films, and Low dimensional systems 6 (1) Summer and Autumn (2022) 603-612

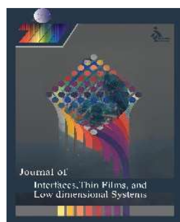

Preparation of ZnO films using metallic Zinc thin layers: the effect of oxidation temperature and substrate type

Scientific research paper

Reza Torkamani, Bagher Aslibeiki*, Hamid Naghshara, Masih Darbandi

Faculty of Physics, University of Tabriz, Tabriz, Iran

ARTICLE INFO

Article history:
Received 30 January 2023
Revised 14 April 2023
Accepted 6 May 2023
Available online 29 June 2023

Keywords
ZnO
Thin film
Sputtering
Substrate
Optical properties

ABSTRACT

In this study, the effect of oxidation temperature and substrate type on the morphology and optical properties of the ZnO films are investigated. The films have been prepared by oxidation of metallic zinc layer under air atmosphere. To examine the effect of oxidation on the growth process, the temperatures of 400, 600, and 800 °C have been considered. To study the impact of the substrate, amorphous quartz and crystalline silicon substrates are used. At 400 °C and quartz substrate, the thin layer grows in the form of particles, while it grows in the nanoflake-like shape when using silicon substrate. The surface roughness increases by increasing the oxidation temperature. The samples prepared on silicon substrate indicate higher surface roughness than those prepared using quartz substrate. The band gap energy of the films elevate by increasing the oxidation temperature from 400 to 600 °C, before decrease by further increasing the annealing temperature to 800 °C. The photoluminescence (PL) spectra of the films confirm the emission due to exciton recombination related to near band edge emission (NBE) and emission due to defects.

1 Introduction

In recent years, zinc oxide (ZnO) has attracted significant attention because of its wide energy gap (3.37 eV) [1], high refractive index [2], ultraviolet absorption [3], the exciton binding energy (60 meV), piezoelectric behavior [4] high photocatalytic performance [5], etc. Therefore, researchers have prepared various ZnO nanostructures, such as nanoparticles [1], nanorods [6], thin film [7], etc., to obtain desired optimal conditions for various applications. Unique features of nanostructural ZnO lead to the development of functional materials for applications in gas sensors [8], water splitting [9], nanogenerators [4], photodiodes, pollutant degradation [5], etc. The ZnO thin films are prepared by different methods such as sputtering [10], spin coating [8], immersion [11], etc. The high-tech sputtering method yields uniform and homogeneous layers [12]. There are various parameters, such as substrate type, temperature, coating rate, sputtering power and gas flow, which are controlled to determine the optimal preparation conditions. Habibi et al. [7] prepared a layer of Zn metal on the quartz substrate using the sputtering method. They prepared ZnO film by oxidation of the Zn metallic layers at different annealing temperatures. They found that at low oxidation temperatures, the thin layer of Zn is not completely oxidized. Moreover, at high temperatures above 1000 °C, the crystalline structure of ZnO film changes from hexagonal to cubic. Gonzalez et al. [10] prepared ZnO films by sputtering method under different deposition rates. They found that by increasing

*Corresponding author.
Email address: b.aslibeiki@Tabrizu.ac.ir
DOI: 10.22051/jitl.2023.42759.1080

the deposition time, the thin films grow along the (002) direction and demonstrate higher roughness. In addition, they found optimal coating time of 9 to 36 min to yield uniform layers with low surface roughness. Therefore, different parameters show a significant impact on the physical properties of thin films. On the above basis, we prepared ZnO films by the sputtering method using Zn metallic target and Si wafer and quartz as substrates. The effect of different annealing temperatures on the oxidation process, morphology, and optical properties of the films was investigated.

2 Materials and methods

2.2 Preparation of thin films

Three amorphous quartz and three crystalline silicon substrates, each with dimensions of 12 x 12 mm, were prepared. First, all the substrates were ultrasonically washed using acetone and ethanol for 10 min. Then, the substrates were placed inside the sputtering chamber (model: Mega2000). The sputtering was started using Zn target and Ar as sputter gas, and the working pressure of 2×10^{-3} mbar. The coating rate was set to 0.8 $Å.s^{-1}$ under the power of 80 W before the Zn metal layer was coated on the substrates with a thickness of 60 nm. After finishing the sputtering process, the samples with quartz substrate were annealed at temperatures of 400 (TQ400), 600 (TQ600), and 800 °C (TQ800) in ambient conditions for 3 h. The annealing process was repeated for the silicon substrates (TSi400, TSi600, and TSi800 for annealing temperatures of 400, 600, and 800 °C, respectively).

2.3 Characterizations

To study the morphology of the samples, X-ray diffraction (XRD) diffractometer model: Siemens D500 and Tongda TD-3700 with wavelength radiation (λ = 1.5406 Å) and a field emission scanning electron microscope (FESEM) model: MIRA3-TESCAN, was used. An atomic force microscope (Model: Nanosurf) was used to study the effect of annealing temperature and substrate on surface roughness and topography. The optical characterizations of the films were performed using an ultraviolet-visible (UV-Vis) spectrometer, Shimadzu model UV-2450, and a photoluminescence (PL) spectrometer JASCO model FP-6200.

3 Results and discussion

3.1 Structural and morphological properties

Figures 1a and 1b indicate the X-ray diffraction patterns of quartz and silicon substrates, respectively. According to Fig. 1a, the quartz substrate shows a broad peak at a range of 15 to 30 degrees where no other peak can be seen. The broad peak indicates that the quartz substrate is amorphous. In addition, Fig. 1b exhibits a sharp peak. This peak demonstrates that the silicon substrate is monocrystalline and shows the peak of the Bragg peak (100) [13].

Figure 2 illustrates FESEM images of prepared ZnO films with quartz and silicon substrates and their particle size distribution at different annealing temperatures. According to the figure, at the annealing temperature of 400 °C, the thin layer is not uniform and shows some cracks. Non-uniformity can indicate that the thin layer of zinc is not entirely oxidized at 400 °C [7]. On the other hand, by increasing the annealing temperature to 600 °C, the thin layer is uniform, and as a result, the metal layer is entirely oxidized. According to the particle size distribution diagrams (inset in Fig. 2), with the elevate of the annealing temperature from 400 to 600 °C, there is no change in the particle size. Meanwhile, the thin layer goes through the oxidation process. The average particle size increases as the annealing temperature ascends to 800 °C. In addition, at this temperature, it loses its uniformity, and the particles stick together. As a result, the annealing temperature of 600 °C is the optimal temperature to obtain a uniform layer with almost monodisperse particle size. The FESEM images of films with Si substrate indicate that the sample with an annealing temperature of 400 °C has a nanoflake-like shape. At this temperature, the nucleation process creates a uniform layer of silicon in the form of nanoflake. At this temperature, the thin zinc oxide layer is not completely oxidized, and only some parts can create islands to form a uniform layer. According to Fig. 2, at 600 °C, the thin layer is completely uniform [14]. At 600 °C, the thin layer of zinc is oxidized, which is the optimal temperature to achieve a uniform layer of ZnO on the silicon substrate. The ZnO thin film loses its uniformity by increasing the annealing temperature to 800 °C and some cracks appear in its structure. The films prepared on the silicon substrate had different growth processes and showed

distinct morphologies compared to those prepared on the quartz substrate. According to Fig. 1, the quartz and silicon substrates were amorphous and monocrystalline, respectively. Therefore, the different morphologies of thin layers can be attributed to the crystalline or amorphous nature of the substrates, which results in a different lattice mismatch. As a result, The lattice mismatch parameter is a possible reason for this difference [15]. EDX spectra were performed to evaluate the stoichiometry of the elements in the samples and ensure the absence of impurities. For example, Fig. 3 shows the spectra of films with an annealing temperature of 600 °C for both substrates. The presence of Zn, O, and Si elements was confirmed. The Si element appeared in the spectra due to the quartz and silicon substrate. The Au element is also seen in the spectra due to the gold coating process for imaging. In addition, the sample TSi600 has a non-stoichiometric structure, but the sample TQ600 has a stoichiometric structure with stoichiometric ratio of 1:1.

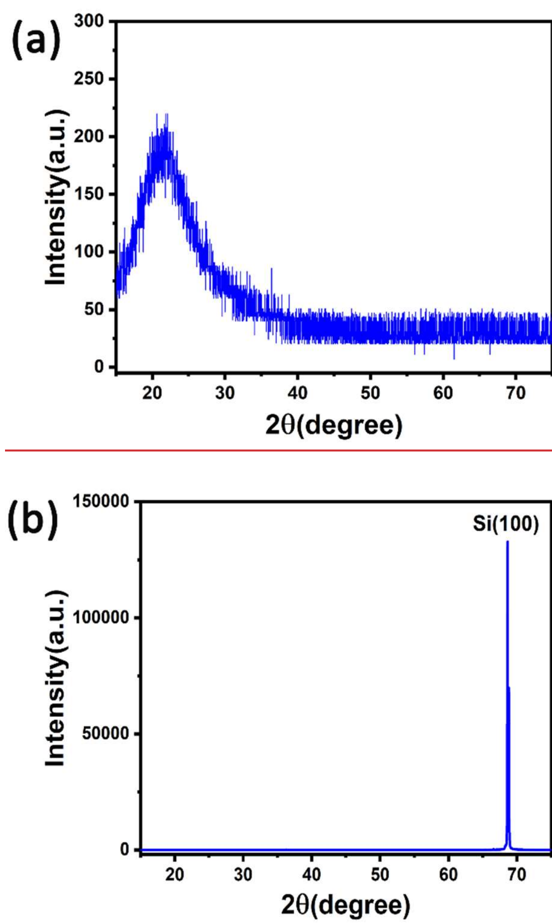

Figure 1. XRD pattern of ZnO films with (a) the quartz and (b) silicon substrates.

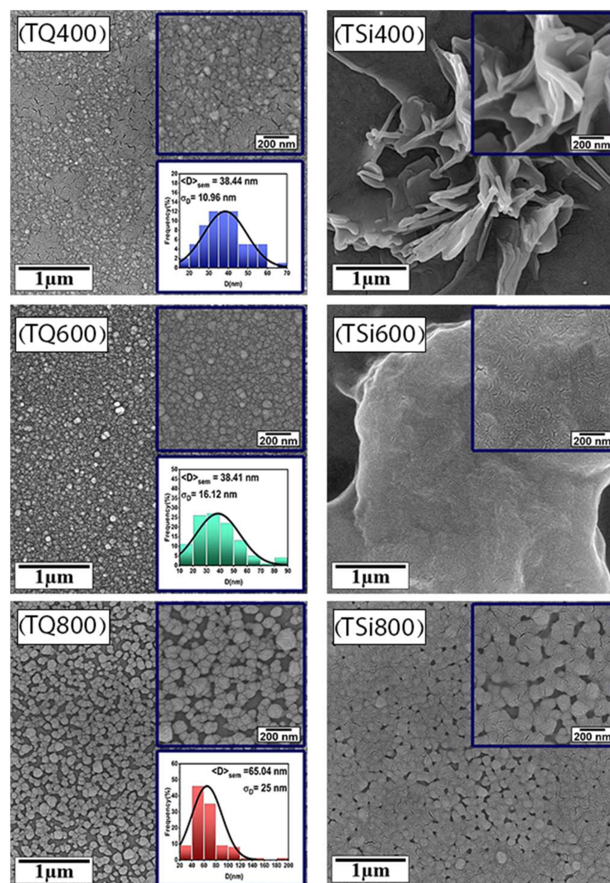

Figure 2. FESEM images of ZnO films with the quartz and silicon substrates.

Figure 4 illustrates the AFM images of quartz and silicon substrates. According to the 2D and 3D images, the substrates have a uniform surface and quartz has a lower height than silicon. Also, according to the surface topography of the substrates, it can be seen that silicon has a surface with higher roughness and height than quartz. The roughness values and surface height of the substrates are indicated in Table 1. According to the table, it can be noted that almost two substrates have the same roughness and height, and as a result, they have the same uniformity.

Figure 5 shows two-dimensional images of the samples measured by atomic force microscopy. According to the figure, for samples with quartz substrate, the surface structure in the sample with an annealing temperature of 400 °C differs from other samples. When the annealing temperature reaches 600 and then 800 °C, a uniform layer is observed. As explained before, at the annealing temperature of 400 °C, the sample is not entirely oxidized, and at the annealing temperature of 600 °C, the layer is completely oxidized. Therefore, the

results obtained from the atomic force microscope images for samples with quartz substrate agree with the scanning electron microscopy.

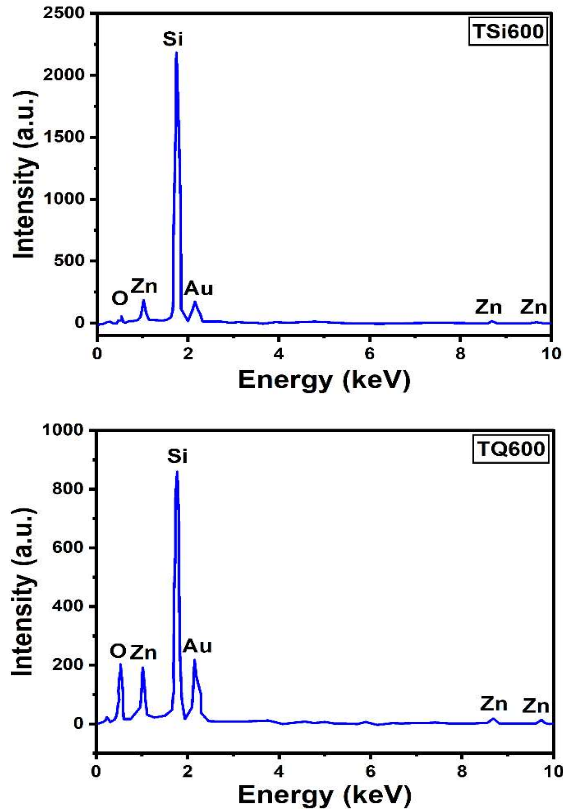

Figure 3. EDX spectra of the samples with an annealing temperature of 600 °C.

Table 1. Average surface roughness and peak-to-valley height in substrates and samples.

Sample	Average surface roughness (nm)	Peak-to-valley height (nm)
Quartz	0.37	2.28
Silicon	0.56	2.83
TQ400	0.59	8.24
TQ600	5.38	68.31
TQ800	9.92	96.78
TSi400	4.50	51.35
TSi600	5.53	61.15
TSi800	46.01	355.90

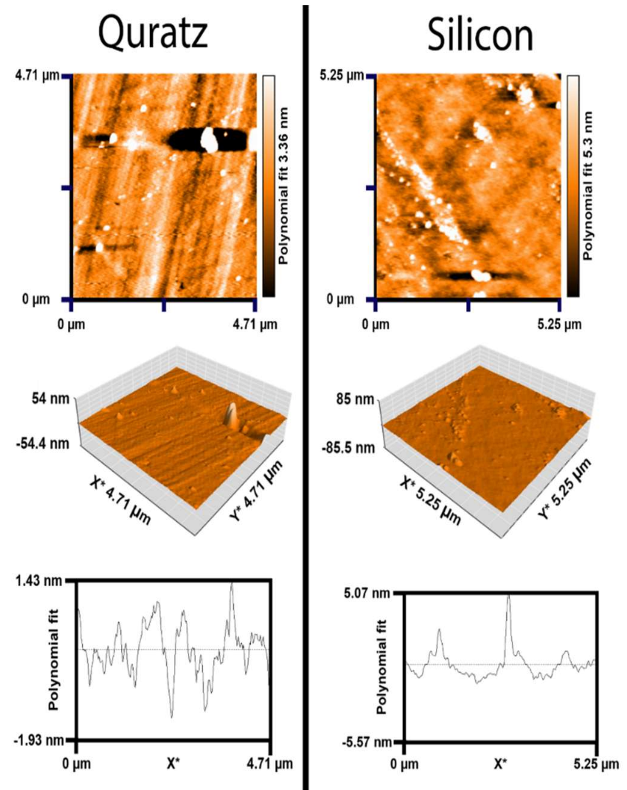

Figure 4. Two-dimensional, 3D, and surface topography of substrates.

According to Figure 5, for the films prepared on the silicon substrate with an annealing temperature of 400 °C, less uniformity is seen compared to other samples. The thin layer becomes uniform by increasing the annealing temperature to 600 °C. Further, by increasing the annealing temperature to 800 °C, the surface structure of the thin layer changes. At this temperature, the silicon substrate is oxidized and forms a layer of SiO_2 between the ZnO and the substrate which will be discussed in the next section.

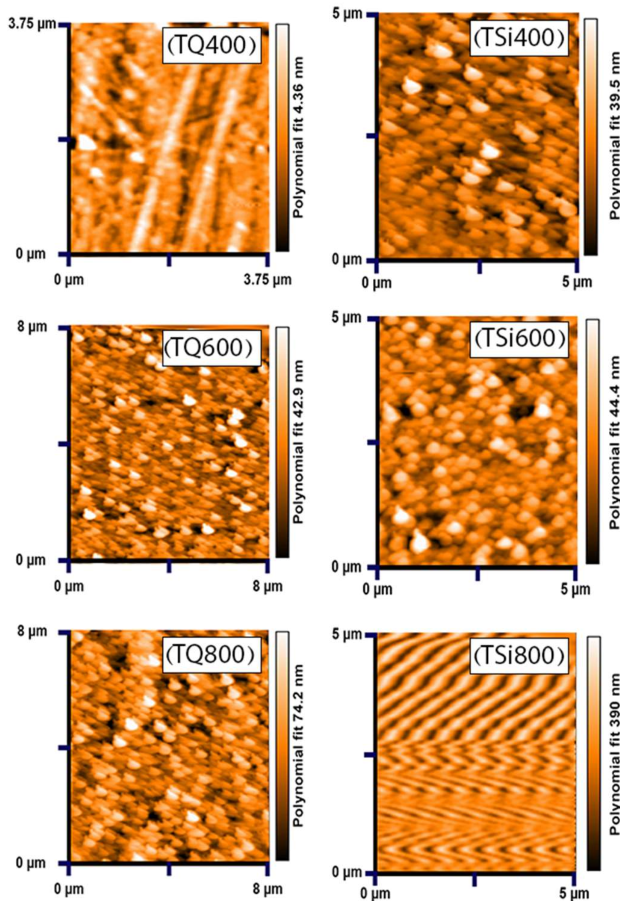

Figure 5. Two-dimensional AFM images of ZnO films with the quartz and silicon substrates.

In Figure 6, three-dimensional AFM images of the samples are shown. As seen from the figure and Table 1, the films with quartz substrate exhibit lower heights than those prepared on the silicon substrate. One possible reason for this difference is the formation of a SiO_2 layer between the ZnO and the substrate. In Fig. 7, the surface topography of the films is illustrated. According to the figure, the peaks-to-valley height of the films ascends with increasing the annealing temperature (see Table 1).

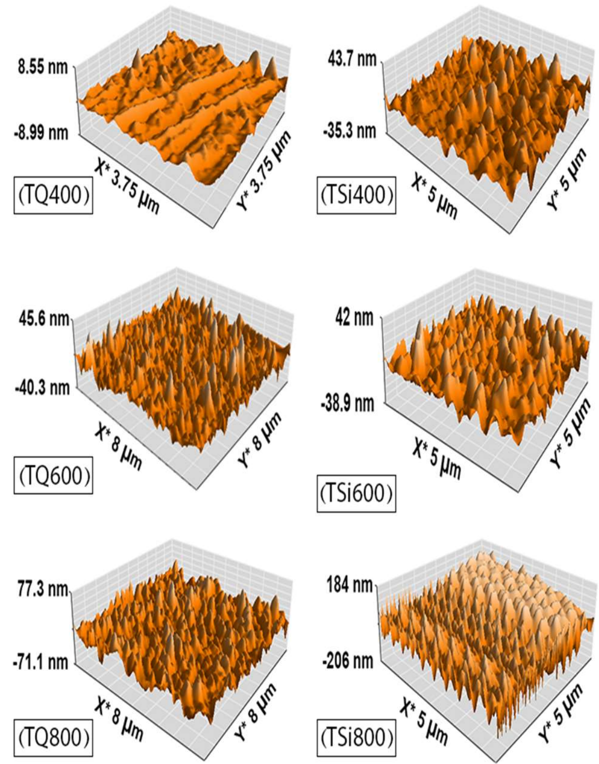

Figure 6. 3D AFM images of ZnO films with the quartz and silicon substrates.

3.2 The reason for the color change of films prepared on the silicon substrate

Figure 8 depicts the thermal oxidation of the metallic zinc layers in the presence of oxygen gas. After the deposition of a thin zinc layer on the substrates, the samples were placed in a furnace. According to the figure, the zinc layer is not completely oxidized at 400 °C. In the sample with silicon substrate, a part of the substrate is oxidized and a SiO_2 thin layer is formed between the zinc layer and the substrate. On the other hand, with ascending the temperature from 400 to 600 and then 800 °C, the metallic zinc layer is completely oxidized.

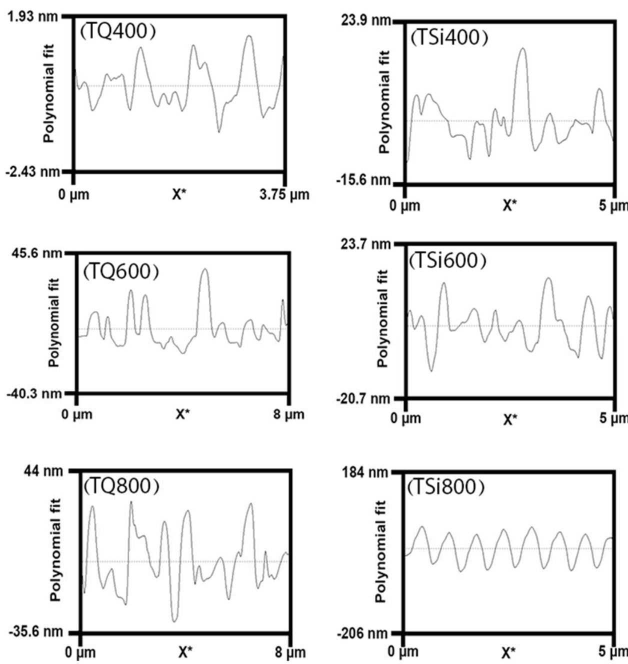

Figure 7. Surface topography of ZnO films with the quartz and silicon substrates.

In the sample with silicon substrate, the thickness of the SiO_2 thin layer elevates with increasing the annealing temperature. Figure 9 shows the images of the samples. As can be seen, the films prepared on the quartz substrate are transparent. Their transparency increases with the increasing annealing temperature. This indicates that with the rise of the annealing temperature, the layer completes the oxidation process and becomes re-crystallized with a perfect crystal structure. On the other hand, as it is clear from Fig. 7, the films prepared on Si substrate show different colors. The reason for this is the growth of a thin layer of SiO_2 between the ZnO layer and the silicon substrate. According to Figure 10, the thin layer of SiO_2 can be changed and seen in different colors according to different thicknesses [16]. On the other hand, as the ZnO film is transparent, the color of silicon is as shown in Fig. 9 (corners of the substrate).

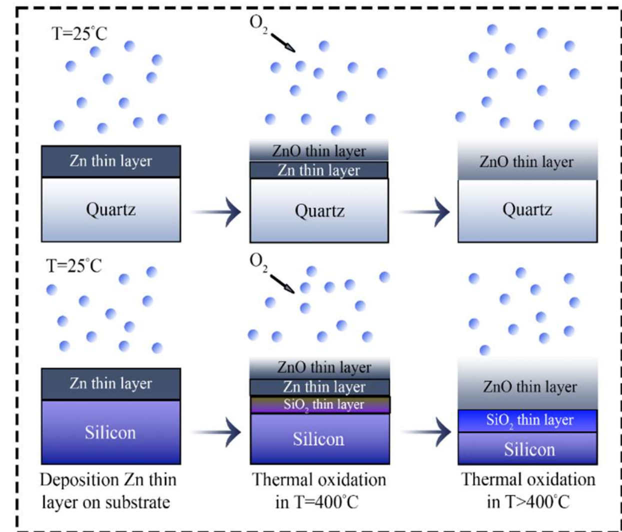

Figure 8. The thermal oxidation process of the metallic zinc layer at different annealing temperatures.

In the sample with an annealing temperature of 400 °C, the sides of the substrate, which does not include the film, remained unchanged in color (see Fig. 9). Nevertheless, in the part where the film is present, a color change is observed. A small amount of the silicon substrate has been oxidized and turned into a thin layer of SiO_2 due to the pressure and temperature applied on the thin film. Because the color of the thin layer of SiO_2 changes by thickness, it can be concluded that a thin layer of SiO_2 is formed between the substrate and the ZnO. As the temperature increases, more silicon is oxidized and turns into a thin layer of SiO_2. In addition, according to Fig. 9, the color of the corners of the substrate did not change at the annealing temperatures of 400 and 600 °C but at the annealing temperature of 800 °C. As a result, considering that the layer of SiO_2 grows between the ZnO and the silicon substrate, the average surface roughness in these samples will be higher than in the samples with quartz substrate. It can also be mentioned that in samples with the quartz substrate, the substrate is not oxidized and does not affect the thin layer of zinc oxide.

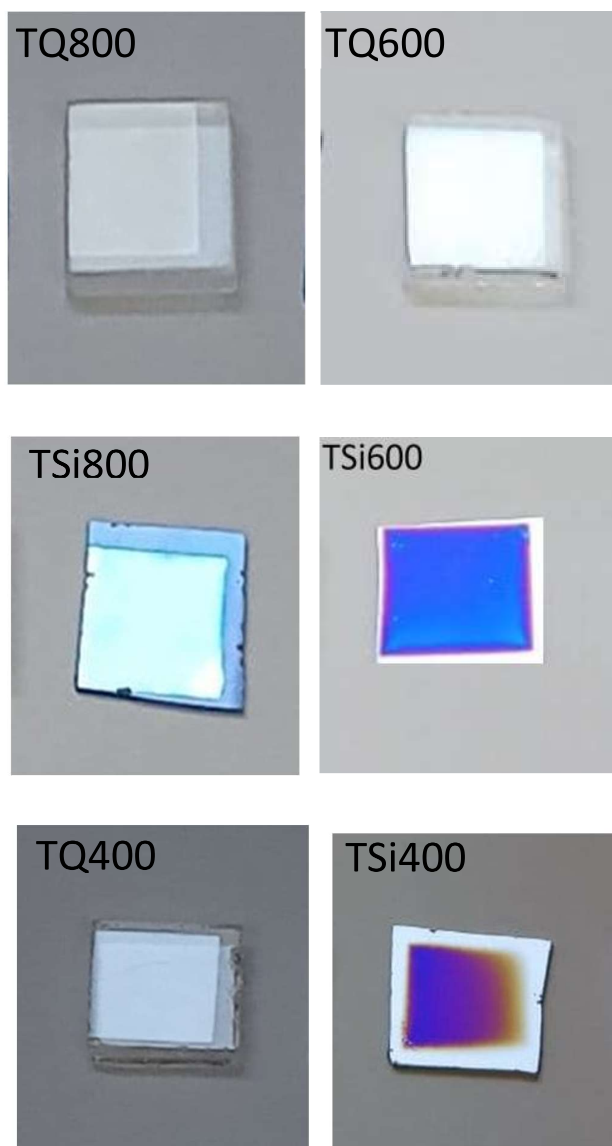

Figure 9. Images of the ZnO films prepared in this research.

3.3 Optical Properties

Figure 11 shows the absorption spectrum and band gap calculated for samples with quartz substrate. As can be seen, no absorption is observed from the wavelength of 400 to 600 nm, which indicates the transparency of the thin films that transmits light in the visible region. In addition, the transparency of these samples in the visible region is shown in Fig. 9. This spectrum confirms the previous statements.

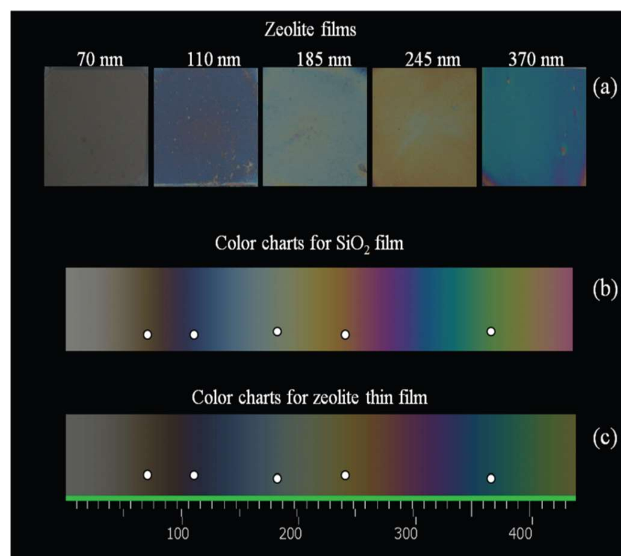

Figure 10. Color charts for SiO_2 (b) film with different thicknesses, image from ref [15].

In the range of 300 to 400 nm, an increase in absorption occurs with decreasing the wavelength. The reason for this is radiation absorption caused by direct transitions of electrons, which can indicate the directness of the band gap [17]. In this research, the Tauc method was used to calculate the band gap energy of the samples. The Tauc equation is given as [18]:

$$(\alpha h\upsilon)^{\frac{1}{n}} = A(h\upsilon - E_g), \quad (1)$$

where the parameter α is the absorption coefficient, A is a constant value, $h\upsilon$ is the incident photon energy, and E_g is the band gap energy. The ZnO has a direct band gap, while n is 0.5. In Fig. 11, the energy gap of the samples is shown. The E_g for the films with annealing temperatures of 400, 600, and 800 °C was obtained as 3.227, 3.232, and 3.050 eV, respectively. The band gap elevates by increasing the annealing temperature from 400 to 600 °C. According to the FESEM images, the sample annealed at 400 °C is not uniform, and by ascending the temperature to 600 °C, a uniform layer was obtained. Therefore, the increase in the band gap can be attributed to the uniformity of the film. When the layer is wholly oxidized at 600 °C, the grain boundaries grow [7]. On the other hand, with the growth of grain boundaries, the band gap ascends. As a result, the increase in the E_g by increasing the temperature from 400 to 600 °C could signify the growth in grain boundaries. On the other hand, the film prepared at

800 °C shows the lowest band gap. As we have seen in Fig. 2, the increase in the average particle size could be the main reason for the decrease in the *Eg* in the sample annealed at 800 °C. Also, with the elevate in grain size, the amount of defect in the structure increases and these defects can affect the energy band gap.

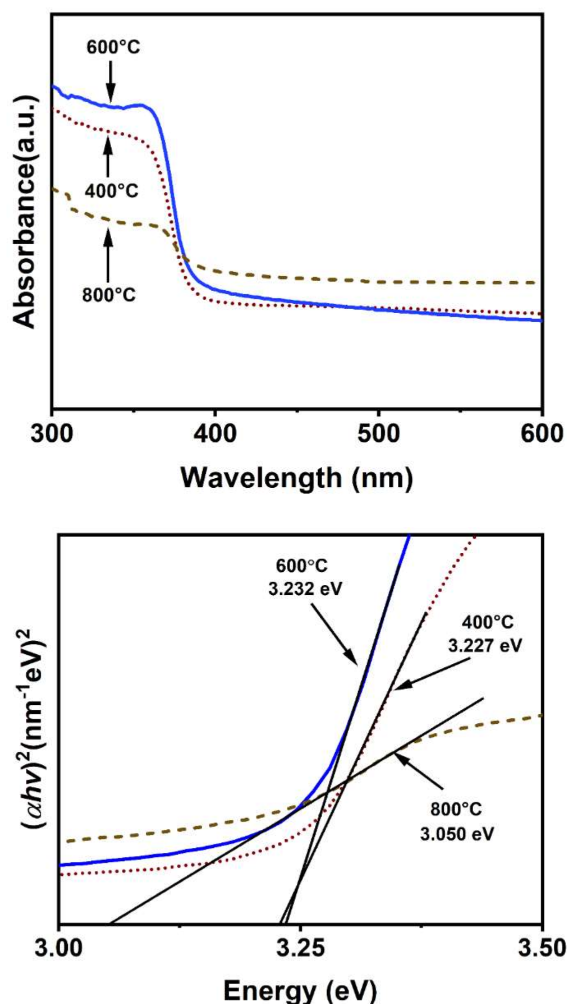

Figure 11. Absorption spectra and band gap energy of ZnO films with the quartz substrate.

Figure 12 indicates the PL spectra of the films with quartz and silicon substrates and their Gaussian fit. In addition, the position of the peaks obtained from Gaussian fitting for each sample is collected in Table 2. We examine the PL spectra of films prepared on the quartz substrate. According to Table 2, the peaks at 386, 385, and 384 nm for the samples with annealing temperatures of 400, 600, and 800 °C, respectively, refer to exciton recombination related to near band edge emission (NBE) [19]. By comparing the NBE values of samples with the energy band gap, TQ800 is expected to have a lower value than other samples. This movement can be caused by the Stokes shift [20]. The peaks located at 459, 465, and 462 nm are due to the emission caused by interstitial zinc atoms (Zn_i) [21], and the peaks located at 404 and 409 nm are related to the vacancy of zinc atoms (V_{Zn}) in the crystal structure [22].

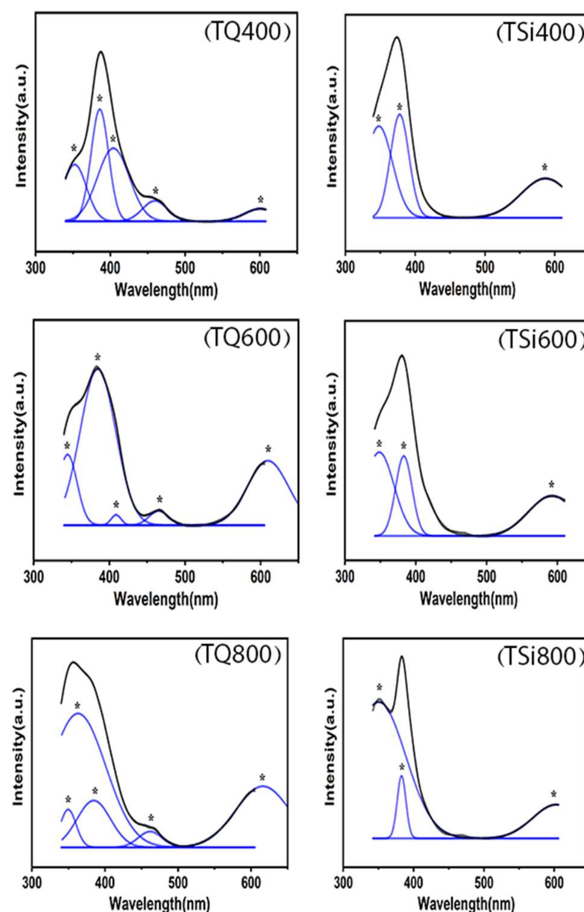

Figure 12. PL spectra of ZnO films with the quartz and silicon substrates.

The peaks at 601, 609, and 616 nm refer to emission through electron transfer from the conduction band to interstitial oxygen atoms (Oi) [23, 24]. As can be seen from Table 2, the peaks located at 377, 383, and 383 nm for the samples with silicon substrate and annealing temperatures of 400, 600, and 800 °C, respectively, refer to NBE. Also, the peaks at 586, 592, and 602 nm refer to Oi in the crystal structure [23, 24]. According to the PL spectra of the samples, the intensity of the NBE peaks is higher than the intensity of the peaks caused by crystal defects. Therefore, it can be concluded that the

samples have a high crystalline structure and fewer crystal defects.

Table 2. The position of PL peaks of ZnO films with the quartz and silicon substrates.

Sample	NBE(nm)	Zn_i - V_{Zn}(nm)	O_i (nm)
TQ400	386	404	601
TQ600	385	409	609
TQ800	384	462	616
TSi400	377	-	586
TSi600	383	-	592
TSi800	383	-	602

4 Conclusions

In this research, ZnO thin films were prepared using the sputtering method, and the effect of substrate and oxidation temperature were investigated. The surface roughness and peak-to-valley height of samples increase with increasing the oxidation temperature. The value of these parameters in the films with the silicon substrate is higher than those prepared on the quartz substrate. From the optical measurements, the emission caused by NBE was confirmed in the films, and crystal defects were observed. The greater intensity of the NBE peaks compared to the peaks related to the defects confirmed the high quality of the films. The increase in the band gap energy in the film annealed at 600 °C is due to the growth of grain boundaries and uniformity of this sample.

References

[1] C. B. Ong, L. Y. Ng, A. W. Mohammad, "A review of ZnO nanoparticles as solar photocatalysts: Synthesis, mechanisms and applications." Renewable and Sustainable Energy Reviews, **81** (2018) 536.

[2] M. Al-Kuhaili, S. Durrani, A. El-Said, R. Heller, "Enhancement of the refractive index of sputtered zinc oxide thin films through doping with Fe_2O_3." Journal of Alloys and Compounds, **690** (2017) 453.

[3] M. A. Khan, M. K. Singha, K. K. Nanda, S. B. Krupanidhi, "Defect and strain modulated highly efficient ZnO UV detector: temperature and low-pressure dependent studies." Applied Surface Science, **505** (2020) 144365.

[4] A. T. Le, M. Ahmadipour, S. Y. Pung, "A review on ZnO-based piezoelectric nanogenerators: Synthesis, characterization techniques, performance enhancement and applications." Journal of Alloys and Compounds, **844** (2020) 156172.

[5] K. Qi, X. Xing, A. Zada, M. Li, Q. Wang, S. Y. Liu, H. Lin, G. Wang, "Transition metal doped ZnO nanoparticles with enhanced photocatalytic and antibacterial performances: experimental and DFT studies." Ceramics International, **46** (2020) 1494.

[6] L. Xu, X. Wang, L. Qian, Y. Zhu, X. Luo, W. Wang, X. Xu, J. Xu, "The dependence of the optical properties of ZnO nanorod arrays on their growth time." Optik, **202** (2020) 163634.

[7] A. Habibi, L. Vatandoust, S. M. Aref, H. Naghshara, "Formation of high performance nanostructured ZnO thin films as a function of annealing temperature: structural and optical properties." Surfaces and Interfaces, **21** (2020) 100723.

[8] N. B. Patil, A. R. Nimbalkar, M. G. Patil, "ZnO thin film prepared by a sol-gel spin coating technique for NO_2 detection." Materials Science and Engineering: B, **227** (2018) 53.

[9] R. Gill, S. Ghosh, A. Sharma, D. Kumar, V. H. Nguyen, D. V. N. Vo, T. D. Pham, P. Kumar, Vertically aligned ZnO nanorods for photoelectrochemical water splitting application, Materials Letters, **277** (2020) 128295.

[10] R. Gonçalves, P. Barrozo, G. Brito, B. Viana, F. Cunha, "The effect of thickness on optical, structural and growth mechanism of ZnO thin film prepared by magnetron sputtering." Thin Solid Films, **661** (2018) 40.

[11] O. Urper, N. Baydogan, "Effect of Al concentration on optical parameters of ZnO thin film derived by Sol-Gel dip coating technique." Materials Letters, **274** (2020) 128000.

[12] X. Zhao, K. Nagashima, G. Zhang, T. Hosomi, H. Yoshida, Y. Akihiro, M. Kanai, W. Mizukami, Z. Zhu, T. Takahashi, "Synthesis of monodispersedly sized ZnO nanowires from randomly sized seeds." Nano Letters, **20** (2019) 599.

[13] T. T. K. Chi, N. T. Le, B. T. T. Hien, D. Q. Trung, N. Q. Liem, "Preparation of SERS substrates for the detection of organic molecules at low concentration." Communications Physics, **26** (2016) 261.

[14] S. Noothongkaew, S. Pukird, W. Sukkabot, B. Kasemporn, P. Songsiririttikul, K. S. An, "Zinc oxide nanostructures synthesized by thermal oxidation of zinc powder on Si substrate." Applied Mechanics and Materials, **328** (2013) 710.

[15] A. Peguit, R. Candidato, F. Bagsican, M. Odarve, M. Jabian, B. Sambo, R. Vequizo, A. Alguno, "Growth of chemically deposited ZnO and ZnO-SiO_2 on Pt buffered Si substrate." IOP Conference Series: Materials Science and Engineering, IOP Publishing, **79** (2015) 012026.

[16] T. Babeva, H. Awala, M. Vasileva, J. El Fallah, K. Lazarova, S. Thomas, S. Mintova, "Zeolite films as building blocks for antireflective coatings and vapor responsive Bragg stacks." Dalton Transactions, **43** (2014) 8868.

[17] K. Vanheusden, C. Seager, W. T. Warren, D. Tallant, J. Voigt, Correlation between photoluminescence and oxygen vacancies in ZnO phosphors, Applied physics letters, **68** (1996) 403.

[18] S. Al-Ariki, N. A. Yahya, S. A. Al-A'nsi, M. Jumali, A. Jannah, R. Abd-Shukor, "Synthesis and comparative study on the structural and optical properties of ZnO doped with Ni and Ag nanopowders fabricated by sol gel technique." Scientific Reports, **11** (2021) 1.

[19] S. Arya, P. Mahajan, S. Mahajan, A. Khosla, R. Datt, V. Gupta, S. J. Young, S. K. Oruganti, "Influence of processing parameters to control morphology and optical properties of Sol-Gel synthesized ZnO nanoparticles." ECS Journal of Solid State Science and Technology, **10** (2021) 023002.

[20] F. Shan, G. Liu, W. Lee, B. Shin, "Stokes shift, blue shift and red shift of ZnO-based thin films deposited by pulsed-laser deposition." Journal of crystal growth, **291** (2006) 328.

[21] M. Patra, K. Manzoor, M. Manoth, S. Vadera, N. Kumar, "Studies of luminescence properties of ZnO and ZnO: Zn nanorods prepared by solution growth technique." Journal of Luminescence, **128** (2008) 267.

[22] L. Wang, F. Wu, D. Tian, W. Li, L. Fang, C. Kong, M. Zhou, "Effects of Na content on structural and optical properties of Na-doped ZnO thin films prepared by sol–gel method." Journal of Alloys and Compounds, **623** (2015) 367.

[23] R. Raji, K. Gopchandran, "ZnO nanostructures with tunable visible luminescence: Effects of kinetics of chemical reduction and annealing." Journal of Science: Advanced Materials and Devices, **2** (2017) 51.

[24] N. Erdogan, T. Kutlu, N. Sedefoglu, H. Kavak, "Effect of Na doping on microstructures, optical and electrical properties of ZnO thin films grown by sol-gel method." Journal of Alloys and Compounds, **881** (2021) 160554.